Diffraction at CDF

Konstantin Goulianos, on behalf of the CDF Collaboration
The Rockefeller University, 1230 York Avenue, New York, NY 10065-6399, USA

Abstract
The diffractive program of the CDF collaboration at the Fermilab Tevatron $p\bar{p}$ Collider is reviewed with emphasis on measurements of the diffractive structure function and on exclusive production from Run II at $\sqrt{s}$ =1.96 TeV. Results on cross sections for exclusive dijet production are used to calibrate theoretical estimates for exclusive Higgs production at the Large Hadron Collider.

1 Introduction

The CDF collaboration has been conducting studies of diffractive interactions at the Fermilab Tevatron $p\bar{p}$ collider since 1989, aiming at elucidating the QCD nature of hadronic diffraction [1]. Diffractive interactions are characterized by one or more large rapidity gaps [2], presumed to occur via the exchange of a *Pomeron*, generically defined as a quark/gluon combination carrying the quantum numbers of the vacuum [3]. The diffractive process directly analogous to classical diffraction is elastic scattering. The total cross section is also of interest in testing theoretical models of diffraction, since it is related to the imaginary part of the forward elastic scattering amplitude through the optical theorem. However, the most stringent tests for QCD inspired models of diffraction are provided by inelastic diffraction. In this paper, we review the results on diffraction reported by CDF and discuss their physics significance. These results have been obtained from a comprehensive program spanning two decades, as outlined in the table below.

Run	Sub-Run	Date	$\int$Lum (pb^{-1})	Process
Run I	IØ	1988-1989	5	σ_{el}, σ_{tot}, σ_{el}
	Ia	1992-1993	20	see Fig. 1 (b)
	Ib	1993-1995	100	”
	Ic	1995-1996	10	”
Run II	IIa	2003-2006	1000	see text
	IIb	in progress		

2 Run IØ Results

In Run IØ, CDF measured the elastic, soft single diffractive, and total $p\bar{p}$ cross sections at $\sqrt{s}$ =630 and 1800 GeV. The measurement was performed with the CDF I detector, which during run IØ had tracking coverage out to $|\eta| \sim 7$ and Roman Pot Spectrometers on both sides of the Interaction Point (IP). The normalization was obtained by the luminosity independent method, which is based on simultaneously measuring the total interaction rate, which depends on σ_{tot}, and the elastic scattering differential rate at $t = 0$, which depends on σ_{tot}^2 (optical theorem):

$$\sigma_{tot} \propto \frac{1}{L}\left(N_{el} + N_{inel}\right) \;\&\; \sigma_{tot}^2 \sim \frac{1}{1+\rho^2}\frac{dN_{el}}{dt}|_{t=0} \;\Rightarrow\; \sigma_{tot} = \frac{16\pi}{1+\rho^2}\frac{1}{N_{el}+N_{inel}}\frac{dN_{el}}{dt}|_{t=0}$$

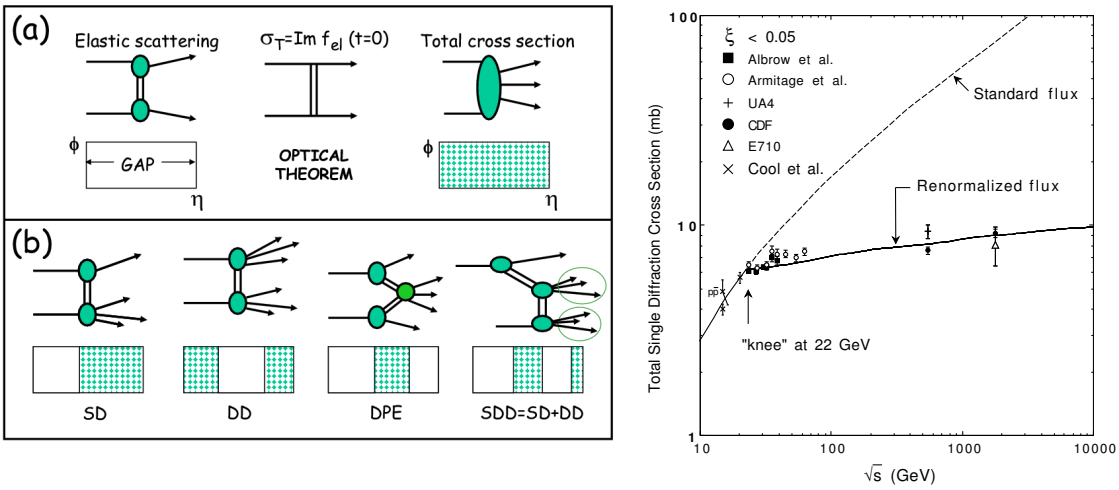

Fig. 1: *(left)* Schematic diagrams and event topologies in azimuthal angle ϕ versus pseudorapidity η for (a) elastic and total cross sections, and (b) single diffraction (SD), double diffraction (DD), double Pomeron exchange (DPE), and double plus single diffraction cross sections (SDD=SD+DD). The hatched areas represent regions in which there is particle production. *(Right)* The total $pp/p\bar{p}$ single diffraction dissociation cross section data (sum of $\bar{p}$ and p dissociation) for $\xi < 0.05$ compared with Regge predictions based on standard and renormalized Pomeron flux [5].

A global Regge fit to total and elastic $p\bar{p}/pp$, $\pi^{\pm}p$, and $K^{\pm}p$ cross sections using the eikonal approach to ensure unitarity yields results consistent with the CDF cross sections even when the CDF results are not used in the fit [4]. In contrast, the standard Regge fit to total single diffractive cross sections, shown in Fig. 1 (*right*), overestimates the Tevatron cross sections by a factor of ~ 10. This discrepancy represents a breakdown of factorization, which is restored by the renormalization procedure proposed in Ref. [5] (see also Ref. [6]).

3 Run Ia,b,c Results

The diffractive processes studied by CDF in Tevatron Runs Ia,b,c are schematically shown in Fig. 1b. Both soft and hard processes were studied. A discussion of the results obtained and of their significance in deciphering the QCD nature of the diffractive exchange can be found in Ref. [7]. The most interesting discoveries are the beakdown of factorization and the restoration of factorization in events with multiple rapidity gaps.

Breakdown of factorization. At $\sqrt{s}$ =1800 GeV, the SD/ND ratios (gap fractions) for dijet, W, b-quark, and J/ψ production, as well the ratio of DD/ND dijet production, are all $\approx 1\%$. This represents a suppression of a factor of $\sim$10 relative to predictions based on diffractive parton densities measured from DDIS at HERA, indicating a breakdown of QCD factorization comparable to that observed in soft diffraction processes relative to Regge theory expectations. However, factorization approximately holds among the four different diffractive processes at fixed $\sqrt{s}$, which indicates that the suppression comes from the formation of the rapidity gap, as predicted by the generalized gap renormalization model (see Ref. [7]).

Restoration of factorization in multi-gap diffraction. Another interesting aspect of the data is that ratios of two-gap to one-gap cross sections for both soft and hard processes obey factorization. This provides both a clue to understanding diffraction in terms of a composite Pomeron and an experimental tool for diffractive studies using processes with multiple rapidity gaps (see Ref. [7]).

4 The Run II Diffractive Program

In Run II, CDF has been conducting the following studies of diffraction:

– structure function in dijet production,

– t distributions,

– exclusive dijet, diphoton [8], and e^+e^- [9] production,

– structure function in W production,

– gap between jets: dependence of the cross section on gap size for fixed $\Delta\eta^{jet}$.

In this paper, we present preliminary results on the diffractive structure function, on diffractive t-distributions, and on exclusive dijet production. The diffractive W and 'gap between jets' analyses are in progress.

4.1 Run II forward detectors

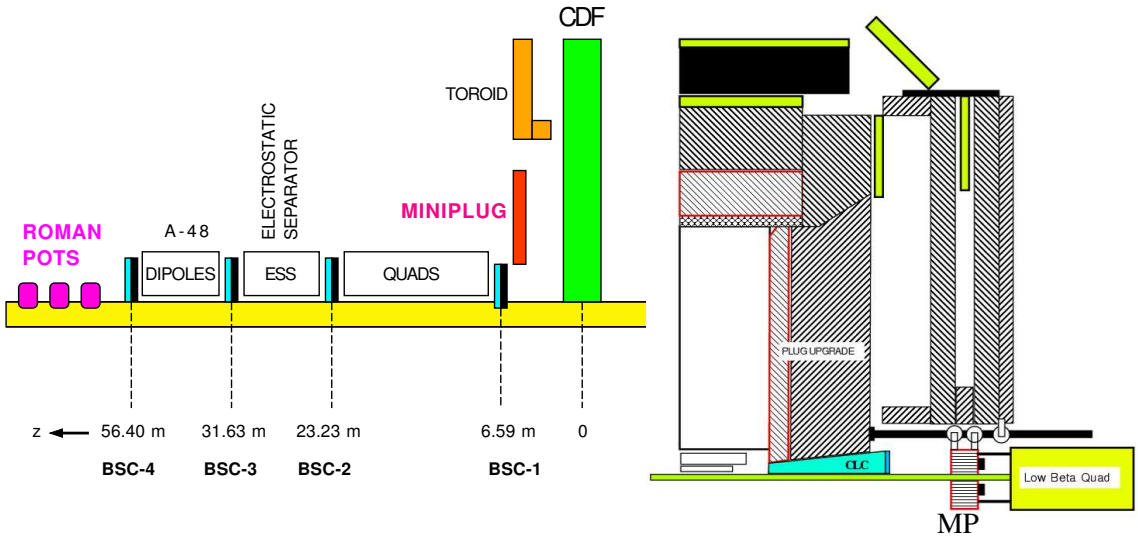

Fig. 2: The CDF detector in Run II: *(left)* location of forward detectors along the $\bar{p}$ direction; *(right)* position of the Cerenkov Luminosity Monitor (CLC) and MiniPlug calorimeters (MP) in the central detector.

The Run II diffractive program was made possible by an upgraded CDF detector [10], which includes the following special forward components (see Fig. 2):

– Roman Pot Spectrometer (RPS) to detect leading antiprotons,

– MiniPlug (MP) forward calorimeters covering the region of $\sim 3.5 < |\eta| < 5.5$,

– Beam Shower Counters (BSC) surrounding the beam pipe within $\sim 5.5 < |\eta| < 7.5$.

The Roman Pot Spectrometer is the same one that was used in Run Ic. It consists of X-Y scintillation fiber detectors placed in three Roman Pot Stations located at an average distance of 57 m downstream in the $\bar{p}$ direction. The detectors have a position resolution of $\pm 100\,\mu m$, which makes possible a $\sim 0.1\%$ measurement of the $\bar{p}$ momentum. In Run Ic, the $\bar{p}$-beam was behind the proton beam, as viewed from the RPS side. An inverted polarity (with respect to Run I) of the electrostatic beam separators enabled moving the RPS detectors closer to the $\bar{p}$-beam and thereby gain acceptance for small $|t|$ down to $\xi \equiv 1 - x_F(\bar{p}) = 0.03$ (for larger $|t|$, lower ξ values can be reached).

The MiniPlug calorimeters are placed within the holes of the muon toroids. They consist of layers of lead plates immersed in liquid scintillator. The scintillation light is picked up by wavelength shifting fibers strung through holes in the lead plates and read out by multi-channel PMT's. The calorimeter "tower" structure is defined by arranging fibers in groups to be read out by individual PMT pixels. There are 84 towers in each MiniPlug measuring energy and position for both electromagnetic and hadron initiated showers [11].

The Beam Shower counters are rings of scintillation counters "hugging" the beam pipe. The BSC-1 rings are segmented into four quadrants, while the other BSCs are segmented into two halves. The BSC-1 are also used to provide rapidity gap triggers and for measuring beam losses.

4.2 Diffractive structure function from dijet production

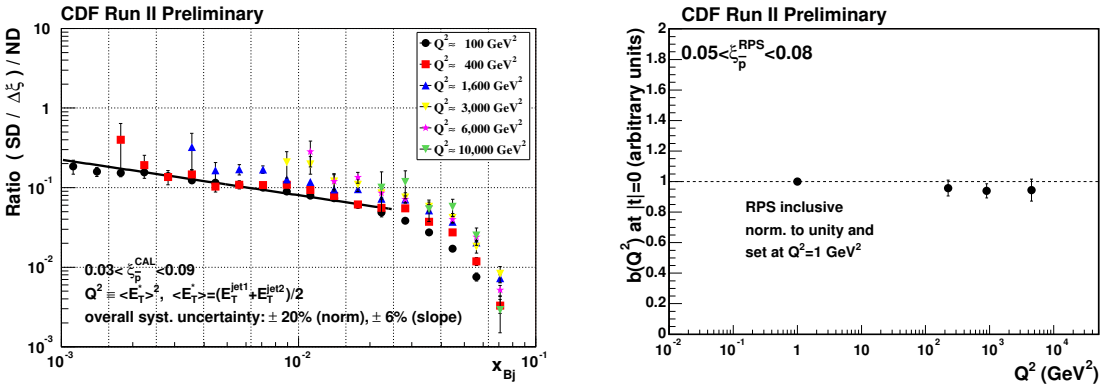

Fig. 3: *(left)* Ratio of diffractive to non-diffractive dijet event rates as a function of x_{Bj} (momentum fraction of parton in antiproton) for different values of $E_T^2 = Q^2$; *(right)* $b|_{t=0}$ slope vs Q^2.

In Run II, CDF has obtained preliminary results for the x_{Bj}, Q^2, and t dependence of the diffractive structure function from dijet production at $\sqrt{s} = 1960$ GeV. The measured x_{Bj} rates confirm the factorization breakdown observed in Run I (see review in Ref. [12]). The Q^2 and t dependence results are shown in Fig 3.

Q^2 **dependence.** In the range 10^2 GeV$^2 < Q^2 < 10^4$ GeV^2, where the inclusive E_T distribution falls by a factor of $\sim 10^4$, the ratio of the SD/ND distribution increases by only a factor of ~ 2. The above results indicate that the Q^2 evolution in diffractive interactions is similar to that in ND interactions.

t**-dependence.** The slope parameter $b(Q^2)|_{t=0}$ of an exponential fit to t distributions near $t = 0$ shows no Q^2 dependence in the range 1 GeV$^2 < Q^2 < 10^4$ GeV^2.

These results support the picture of a composite Pomeron formed from color singlet combinations of the underlying parton densities of the nucleon (see Ref. [7]).

4.3 Exclusive Dijet Production

Exclusive production in $p\bar{p}$ collisions is of interest not only for testing QCD inspired models of diffraction, but also as a tool for discovering new physics. The process that has attracted the most attention is exclusive Higgs boson production. The search for Higgs bosons is among the top priorities in the research plans of the LHC experiments. While the main effort is directed toward searches for inclusively produced Higgs bosons, an intense interest has developed toward exclusive Higgs production, $\bar{p}/p + p \rightarrow \bar{p}/p + H + p$. This Higgs production channel presents several advantages: it can provide clean events in an environment of suppressed QCD background, in which the Higgs mass can accurately be measured using the missing mass technique by detecting and measuring the momentum of the outgoing proton and (anti)proton. However, exclusive production is hampered by expected low production rates [13]. As rate calculations are model dependent and generally involve non-perturbative suppression factor(s), it is prudent to calibrate them against processes involving the same suppression factors(s), but have higher production rates that can be measured at the Tevatron. One such processes is exclusive dijet production, which proceeds through the same mechanism as Higgs production, as shown in Fig. 4.

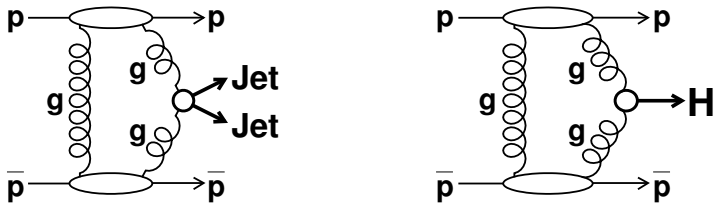

Fig. 4: Lowest order diagrams for exclusive dijet (left) and Higgs (right) production in $\bar{p}p$ collisions.

The search for exclusive dijets is based on measuring the dijet mass fraction, R_{jj}, defined as the mass of the two leading jets in an event, M_{jj}, divided by the total mass reconstructed from the energy deposited in all calorimeter towers, M_X. The signal from exclusive diets is expected to appear at high values of R_{jj}, smeared by resolution and radiation effects. Events from inclusive DPE production, $\bar{p}p \rightarrow \bar{p} + gap + jj + X + gap$, are expected to contribute to the entire M_{jj} region. Any such events within the exclusive M_{jj} range contribute to background and must be subtracted when evaluating exclusive production rates.

The exclusive signal is extracted from the inclusive R_{jj} distribution by fitting the data with MC simulations [14]. Two methods have been used. In the first one, the POMWIG and ExHuME generators are used for simulating inclusive and exclusive events, respectively, while in the second, inclusive (exclusive) distributions are simulated using the POMWIG (DPEMC) program. Experimentally, the MC non-exclusive dijet background shape is checked by a study of high E_T b-tagged dijet events, as quark jet production through $gg \to \bar{q}q$ is suppressed in LO QCD by the $J_z = 0$ selection rule as $m_q/M^{jet} \to 0$.

Figure 5 shows measured R_{jj} distributions plotted versus dijet mass fraction. On the left, the number of events within the specified kinematic region the data are compared with fits based on POMWIG plus ExHuME distribution shapes, and on the right with fits based on POMWIG⊕DPEMC predictions. Both approaches yield good fits to the data. The suppression factor expected for exclusive b-tagged dijet events is checked with CDF data in Fig. 6. Within the quoted errors, this result validates the MC based method for extracting the exclusive signal. In

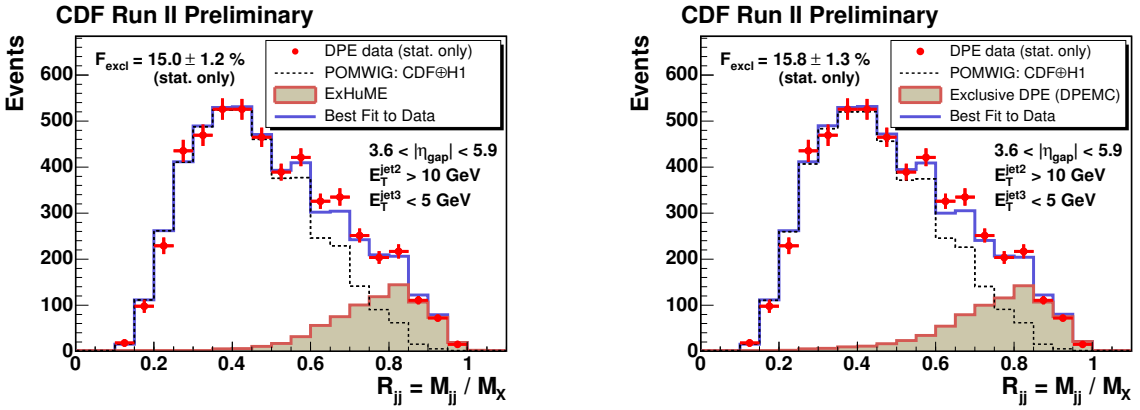

Fig. 5: Extraction of exclusive dijet production signal using Monte Carlo techniques to subtract the inclusive dijet background: *(left)* dijet mass fraction in data (points) and best fit (solid line) obtained from MC events generated using the POMWIG (dashed) and ExHuME (filled) MC generators for inclusive and exclusive events, respectively; *(right)* the same data fitted with POMWIG and exclusive DPEMC generators.

Fig. 7 *(left)*, integrated cross sections above a minimum $E_T^{jet1,2}$ are compared with ExHuME and DPEMC predictions. The data favor the ExHuME prediction. ExHuME hadron level differential cross sections $d\sigma^{excl}/dM_{jj}$, normalized to the measured data points of Fig. 7 *(left)*, are shown in Fig. 7 *(right)* with errors propagated from the uncertainties in the data. Within the errors, the good agreement with the default ExHuME prediction up to masses in the region of the standard model Higgs mass predicted from global fits to electroweak data confirms the calculation of Ref. [13] for exclusive Higgs boson production at the LHC.

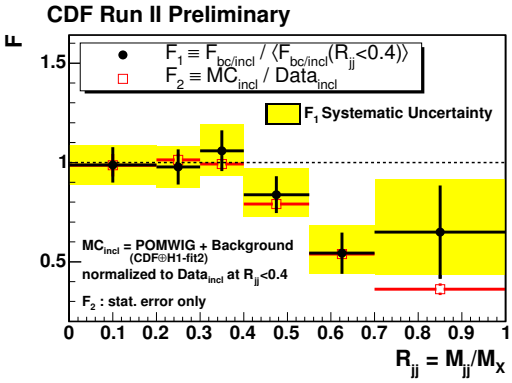

Fig. 6: *(circles)* Fraction of heavy flavor (b, c) to all dijet events in data, F_1, as a function of dijet mass fraction showing the expected suppression at high M_{jj}; *(squares)* fraction, F_2, of inclusive MC to data from Fig. 5 (left). The agreement between the measured suppression levels in F_1 and F_2 serves to validate the MC based technique for extracting the exclusive production rate from the data.

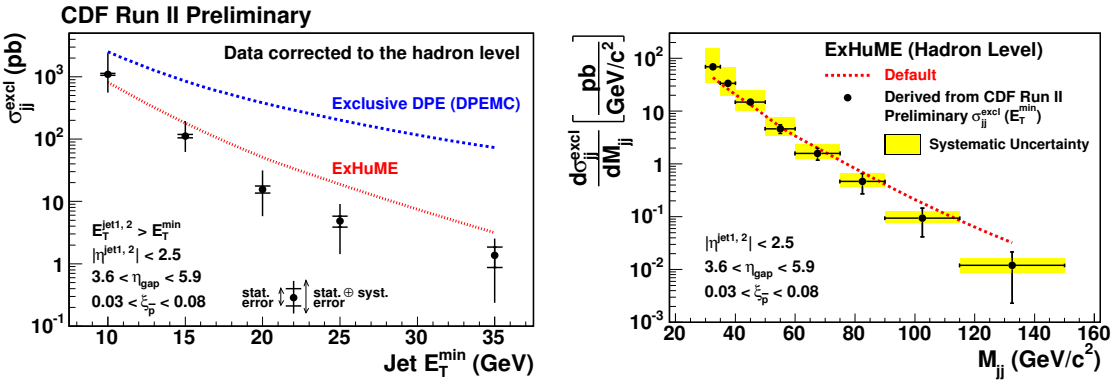

Fig. 7: *(left)* Measured exclusive dijet cross sections versus the minimum E_T of the two leading jets compared with ExHuME and DPEMC predictions; *(right)* ExHuME hadron level differential exclusive dijet cross section vsersus dijet mass normalized to the CDF cross sections at *left*. The systematic errors shown are propagated from those in the data; the ExHuME predictions have comparable systematic uncertainties.

5 Summary

Diffractive processes studied by CDF in Run I include elastic and total cross sections, soft diffractive cross sections with single and multiple rapidity gaps, and hard single diffractive production of dijet, W, b-quark, and J/ψ production, as well as central dijet production in events with two forward rapidity gaps (double Pomeron exchange). The results obtained support a picture of universality of diffractive rapidity gap formation across soft and hard diffractive processes, which favors a composite over a particle-like Pomeron made up from color singlet quark and/or gluon combinations with vacuum quantum numbers.

Run II preliminary results on the x_{Bj} and Q^2 dependence of the diffractive structure function obtained from dijet production are also presented, as well as results on the slope parameter of the t-distribution of diffractive events as a function of Q^2. In the range 10^2 GeV^2 $< Q^2 <$ 10^4 GeV^2, where the inclusive E_T distribution falls by a factor of $\sim 10^4$, the ratio of SD/ND

distributions varies by at most a factor of ~ 2, indicating that the Q^2 evolution in diffractive interactions is similar to that in ND ones. The slope parameter $b(Q^2)|_{t=0}$ of an exponential fit to t distributions near $t = 0$ in the range $1\ \mathrm{GeV}^2 < Q^2 < 10^4\ \mathrm{GeV}^2$ shows no Q^2 dependence. These results support a picture of a composite diffractive exchange (Pomeron) made up from the underlying parton densities of the nucleon [7].

References

[1] See e. g. K. Goulianos, *Diffractive and Total Cross Sections at Tevatron and LHC*, in *Hadron Collider Physics Symposium 2006*, May 22-26, Duke University, Durham, NC, USA.

[2] Rapidity gaps are regions of rapidity devoid of particles; rapidity, $y = \frac{1}{2}\frac{E+p_L}{E-p_L}$, and pseudorapidity, $\eta = -\ln\tan\frac{\theta}{2}$, are used interchangeably in this paper, as in the kinematic region of interest the values of these two variables are approximately equal.

[3] P. D. B. Collins, *An Introduction to Regge Theory and High Energy Physics*, Cambridge University Press (1977); V. Barone and E. Predazzi, *High-Energy Particle Diffraction*, Springer Press (2001); S. Donnachie, G. Dosch, O. Nachtmann, and P. Landshoff, *Pomeron Physics and QCD*, Cambridge University Press (2002).

[4] R. J. M. Covolan, J. Montanha, and K. Goulianos, *A New Determination of the Soft Pomeron Intercept*, Phys. Lett. B **389**, 176 (1996).

[5] K. Goulianos, *Renormalization of Hadronic Diffraction and the Structure of the Pomeron*, Phys. Lett. B **358**, 379 (1995); Erratum-*ib.* **363**, 268 (1995).

[6] K. Goulianos, *Pomeron Intercept and Slope: the QCD Connection*, in these proceedings.

[7] K. Goulianos, *Hadronic Diffraction: Where do we Stand?*, in *La Thuile 2004, Results and Perspectives in Particle Physics*, edited by M. Greco, Proc. of Les Rencontres de Physique de la Vallé d'Aoste, La Thuile, Aosta Valley, Italy, February 29 - March 6, 2004, pp. 251-274; e-Print Archive: hep-ph/0407035.

[8] T. Aaltonen *et al.* (CDF Collaboration), *Search for Exclusive $\gamma\gamma$ Production in Hadron-Hadron Collisions*, FERMILAB-PUB-07-384-E, Jul 2007, e-Print: arXiv:0707.2374 [hep-ex], Submitted to Phys. Rev. Lett.

[9] A. Abulencia *et al.* (CDF Collaboration), *Observation of Exclusive Electron-Positron Production in Hadron-Hadron Collisions*, Phys.Rev.Lett.98:112001,2007, FERMILAB-PUB-06-436-E, Nov 2006, e-Print: hep-ex/0611040.

[10] R. Blair *et al.* (CDF Collaboration), *The CDF II Detector: Technical Design Report*, FERMILAB-Pub-96/390-E.

[11] K. Goulianos and S. Lami, *Performance of a Prototype Position Sensitive Towerless Calorimeter*, *Nucl. Instrum. Meth. A* **430**, 34-47 (1999); K. Goulianos *et al.*, *The CDF MiniPlug calorimeters*, *Nucl. Instrum. Meth. A* **496**, 333-346 (2003).

[12] M. Gallinaro (for the CDF collaboration), *Diffractive and exclusive measurements at CDF*, Presented at 14th International Workshop on Deep Inelastic Scattering (DIS 2006), Tsukuba, Japan, 20-24 Apr 2006; e-Print Archive: hep-ex/0606024.

[13] V. Khoze, A. Kaidalov, A. Martin, M. Ryskin, and W. Stirling, *Diffractive processes as a tool for searching for new physics*, e-Print Archive:hep-ph/0507040, and references therein.

[14] Monte Carlo programs used in the CDF analysis: **POMWIG** (implements diffraction into the HERWIG Monte Carlo Generator) B. Cox and J. Forshaw, *Comput. Phys. Commun.* **144**, 104 (2002); **DPEMC** (extends POMWIG to include inclusive and exclusive DPE) M. Boonekamp and T. Kucs, *Comput. Phys. Commun.* **167**, 217 (2005); **ExHuME** (implements the exclusive dijet production calculation of Ref. [13]), J. Monk and A. Pilkington, e-Print Archive: hep-ph/0502077.